Super-Charged Porphyrazines: Synthesis and Physical Properties of Octacationic Tetraazaporphyrins

Máirín E. Anderson,[†] Anthony G. M. Barrett,[‡] and Brian M. Hoffman*,[†]

Departments of Chemistry, Northwestern University, Evanston, Illinois 60208, and Imperial College of Science, Technology and Medicine, London, England

Received April 14, 1999

We report the synthesis of octacationic macrocycles based on the porphyrazine (tetraazaporphyrin) core. The first stage is the synthesis of Mg(II) 2,3,7,8,12,13,17,18-octakis(4-pyridyl)porphyrazine, [Mgpz(pyr)$_8$], and the parent [H$_2$pz(pyr)$_8$]. Both compounds are freely soluble in aqueous acid due to protonation of the pyridyl groups but with concomitant loss of Mg^{2+} by the latter. Methylation of [H$_2$pz(pyr)$_8$] gives the octacation, 2,3,7,8,12,13,17,18-octakis(*N*-methyl-4-pyridiniumyl)porphyrazine, [H$_2$pz(Me-pyr)$_8$]$^{8+}$, which is freely soluble in water as the chloride salt. The peripheral charges greatly lower the pK_a values of the pyrrole protons of [H$_2$pz(Me-pyr)$_8$]$^{8+}$ in aqueous solution. Global fitting of optical pH titration curves gives pK_a values for the first and second deprotonations of 6.3 and 8.8 in 2.0 M NaCl and 4.1 and 5.6 at 0.1 M NaCl. The analysis further gives the UV−visible spectra of the [H$_2$pz(Me-pyr)$_8$]$^{8+}$, [Hpz(Me-pyr)$_8$]$^{7+}$, and [pz(Me-pyr)$_8$]$^{6+}$ species. The free-base compound [H$_2$pz(Me-pyr)$_8$]$^{8+}$ rapidly incorporates a variety of metal ions (Ba(II), Cd(II), Co(II), Cu(II), Mn(III), Ni(II), Pd(II), and Zn(II)) to form [Mpz(Me-pyr)$_8$]$^{8+}$. We present the complete synthesis and characterization of the [Nipz(Me-pyr)$_8$]$^{8+}$ and [Cupz(Me-pyr)$_8$]$^{8+}$ derivatives.

Introduction

Cationic porphyrinic macrocycles represent a large and expanding class of compounds which have applications in biology, medicine, catalysis, and materials. The classical cationic porphyrin *meso*-tetrakis(*N*-methylpyridiniumyl)porphyrin (TMPyP) first attracted attention as a water-soluble porphyrin that could be studied over a wide pH range;[1] later, TMPyP was recognized to interact with DNA through both outside binding and intercalation.[2] Since then, cationic porphyrins have been investigated as DNA-binding and cleavage reagents,[3] sensitizers for photodynamic therapy,[4] nuclease-resistant delivery agents for antisense oligonucleotides,[5,6] and probes for nucleic acid structure[7] and peptide electron transfer.[8] As catalysts, the manganese derivatives are effective at superoxide dismutation and peroxynitrite decomposition,[9] and sandwich complexes have been synthesized to use as models of the photosynthetic reaction center.[10] Films of cationic porphyrinic macrocycles have shown promise in electrocatalytic reduction of dioxygen,[11] and materials applications such as metal ion[12,13] and sugar sensing[14] have been explored. Supramolecular structures have been assembled,[15] and the properties of these new materials, including nonlinear optical behavior[16] and memory,[17,18] are being investigated.

Cationic tetraazaporphyrins, or porphyrazines, represent an alternative and highly underdeveloped class of cationic por-

[†] Northwestern University.
[‡] Imperial College of Science, Technology and Medicine.

(1) Fleischer, E. B. *Inorg. Chem.* **1962**, *1*, 493−495.
(2) (a) Fiel, R. J.; Howard, J. C.; Mark, E. H.; Datta Gupta, N. *Nucleic Acids Res.* **1979**, *6*, 3093−3118. (b) Carvlin, M. J.; Fiel, R. J. *Nucleic Acids Res.* **1983**, *11*, 6121−6139. (c) Marzilli, L. G. *New J. Chem.* **1990**, *14*, 409−420. (d) Pasternack, R. F.; Gibbs, E. J. *Met. Ions Biol. Syst.* **1996**, *33*, 367−397.
(3) (a) Groves, J. T.; Farrell, T. P. *J. Am. Chem. Soc.* **1989**, *111*, 4998−5000. (b) Sentagne, C.; Meunier, B.; Paillous, N. *J. Photochem. Photobiol. B* **1992**, *16*, 47−59. (c) Mestre, B.; Jakobs, A.; Pratiel, G.; Meunier, B. *Biochemistry* **1996**, *35*, 9140−9149. (d) Pratviel, G.; Bernadou, J.; Meunier, B. *Met. Ions Biol. Syst.* **1996**, *33*, 399−426.
(4) (a) Villanueva, A.; Caggiari, L.; Jori, G.; Milanesi, C. *J. Photochem. Photobiol. B* **1994**, *23*, 49−56. (b) Kessel, D.; Woodburn, K.; Hendersen, B. W.; Chang, C. K. *Photochem. Photobiol.* **1995**, *62*, 875−881. (c) Merchat, M.; Spikes, J. D.; Bertoloni, G.; Jori, G. *J. Photochem. Photobiol. B* **1996**, *35*, 149−157. (d) Cernay, T.; Zimmermann, H. W. *J. Photochem. Photobiol. B* **1996**, *34*, 191−196.
(5) Bigey, P.; Pratviel, G.; Meunier, B. *J. Chem. Soc., Chem. Commun.* **1995**, 181−182.
(6) Benimetskaya, L.; Takle, G. B.; Vilenchik, M.; Lebedeva, I.; Miller, P.; Stein, C. A. *Nucleic Acids Res.* **1998**, *26*, 5310−5317.
(7) (a) Nussbaum, J. M.; Newport, M. E. A.; Mackie, M.; Leontis, N. B. *Photochem. Photobiol.* **1994**, *59*, 515−528. (b) Eggleston, M. K.; Crites, D. K.; McMillin, D. R. *J. Phys. Chem. A* **1998**, *102*, 5506−5511. (c) Anantha, N. V.; Azam, M.; Sheardy, R. D. *Biochemistry* **1998**, *37*, 2709−2714. (d) Arthanari, H.; Basu, S.; Kawano, T. L.; Bolton, P. H. *Nucleic Acids Res.* **1998**, *26*, 3724−3728.
(8) Aoudia, M.; Rodgers, M. A. J. *J. Am. Chem. Soc.* **1997**, *119*, 12859−12868.
(9) (a) Pasternack, R. F.; Halliwell, B. *J. Am. Chem. Soc.* **1979**, *101*, 1026−1031. (b) Liochev, S. I.; Fridovich, I. *Arch. Biochem. Biophys.* **1995**, *321*, 271−275. (c) Lee, J. B.; Hunt, J. A.; Groves, J. T. *J. Am. Chem. Soc.* **1998**, *120*, 6053−6061.
(10) Buchler, J. W.; Nawra, M. *Inorg. Chem.* **1994**, *33*, 2830−2837.
(11) (a) Shi, C.; Anson, F. C. *Inorg. Chem.* **1995**, *34*, 4554−4561. (b) Zhang, J.; Pietro, W.; Lever, A. B. P. *J. Electroanal. Chem.* **1996**, *403*, 93−100. (c) D'Souza, F.; Hsieh, Y. Y.; Deviprasad, G. R. *J. Chem. Soc., Chem. Commun.* **1998**, 1027−1028.
(12) Bellacchio, E.; Gurrieri, S.; Lauceri, R.; Magrì, A.; Scolaro, L. M.; Purrello, R.; Romeo, A. *J. Chem. Soc., Chem. Commun.* **1998**, 1333−1334.
(13) Tabata, M.; Nishimoto, J.; Kusano, T. *Talanta* **1998**, *46*, 703−709.
(14) Arimori, S.; Takeuchi, M.; Shinkai, S. *Chem. Lett.* **1996**, 77−78.
(15) (a) Ojadi, E.; Selzer, R.; Linschitz, H. *J. Am. Chem. Soc.* **1985**, *107*, 7783−7784. (b) Abrahams, B. F.; Hoskins, B. F.; Michail, D. M.; Robson, R. *Nature* **1994**, *369*, 727−729. (c) Drain, C. M.; Lehn, J.-M. *J. Chem. Soc., Chem. Commun.* **1994**, 2313−2315. (d) Komatsu, T.; Yanagimoto, T.; Tsuchida, E.; Siggel, U.; Fuhrhop, J.-H. *J. Phys. Chem. B* **1998**, *102*, 6759−6765.
(16) Si, J.; Wang, Y.; Yang, Q.; Ye, P.; Tian, H.; Zhou, Q.; Xu, H. *Appl. Phys. Lett.* **1996**, *69*, 1832−1834.
(17) Bellacchio, E.; Lauceri, R.; Gurrieri, S.; Scolaro, L. M.; Romeo, A.; Purrello, R. *J. Am. Chem. Soc.* **1998**, *120*, 12353−12354.
(18) Purrello, R.; Scolaro, L. M.; Bellacchio, E.; Gurrieri, S.; Romeo, A. *Inorg. Chem.* **1998**, *37*, 3647.

10.1021/ic990410s CCC: $18.00
Published on Web 12/10/1999

phyrinic compounds. Macrocycles based on the porphyrazine core, including phthalocyanines, exhibit many of the same properties as porphyrins, but the replacement of the *meso* methylene carbons of porphyrins with nitrogen in porphyrazines creates profound differences.[19,20] For example, porphyrazines absorb more strongly at longer wavelengths[19,21]—a critical feature in biological and medical applications. Furthermore, the synthetic route to porphyrazines, which involves cyclization of functionalized maleonitriles, rather than pyrroles, gives opportunities for generating new types of functionalization at the peripheral β-carbons.[22−25] To date, the only multicationic porphyrazines that have been studied involve substitution of the fused benzenes of phthalocyanines with pyridine or pyrazine groups (pyridino- or pyrazinoporphyrazines) or addition of cationic groups to the periphery of the fused benzene rings.[26−28] However, phthalocyanines exhibit a strong tendency to aggregate[28−30] (aggregation severely hinders the reactivity of these compounds for most applications), and in cases of unsymmetrical phthalocyanines it is difficult to separate the isomers.[27] Direct functionalization of the β-pyrrole carbons with pyridyl groups would decrease aggregation and avoid problems of isomer purification while retaining the advantages of the porphyrazine core.

In this paper we report (i) the synthesis and characterization of a porphyrazine that has eight peripheral pyridyl groups and is soluble in aqueous acid and (ii) methylation of the pyridyl groups to give the *octacationic* porphyrazine, which is soluble in water over a wide pH range.

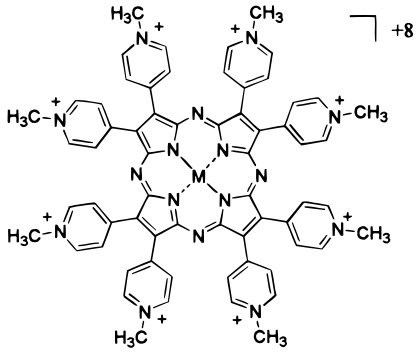

[Mpz(Me-pyr)$_8$]$^{+8}$

Titrations of the octakis(methylpyridyl)porphyrazine in water show that the internal pyrrolic nitrogens have pK_a values lower than any previously reported for phthalocyanines or porphyrins,[13,31−34] and the analysis gives the spectra of the individual $[H_2pz(Me\text{-}pyr)_8]^{8+}$, $[Hpz(Me\text{-}pyr)_8]^{7+}$, and $[pz(Me\text{-}pyr)_8]^{6+}$ species. At ambient temperature and neutral pH, a wide variety of metals can be rapidly complexed within the core of the octakis(methylpyridyl)porphyrazine, and we report details of the properties of two such metal-incorporated species. Finally, aggregation studies confirm the monomeric nature of these novel cationic porphyrazines, making them excellent candidates for a wide variety of applications.

Experimental Section

Materials. 4-Pyridylacetonitrile hydrochloride, methyl 4-toluenesulfonate, Amberlite IRA-400(Cl) ion-exchange resin, iodine, and solvents other than water were purchased from Aldrich and used as received. Water was purified by the Millipore Milli-Q water system before use. Glassware was treated with Plusone Repel-Silane ES (Pharmacia Biotech) before use to prevent the cationic compounds from adsorbing onto the glass. Electronic absorption spectra were recorded in a quartz cuvette using a Hewlett-Packard HP8452A diode array spectrophotometer. A Beckman Φ34 pH meter was used to monitor pH in titration experiments. Fluorescence measurements were obtained on a PTI fluorimeter. ^{1}H NMR experiments were obtained on a Varian Gemini 300 MHz spectrometer. Fast atom bombardment (FAB) mass spectra were recorded locally by Dr. Doris Hung using a VG-70-250SE instrument. Elemental analyses were performed by Oneida Research Services, Whitesboro, NY. Electron paramagnetic resonance (EPR) spectra were measured using a modified Varian E-4 X-band spectrometer. Activated neutral Brockmann standard grade alumina was used in liquid column chromatography.

Methods. Interpretation of UV−Visible Spectra. The electronic absorption spectra of porphyrazines can be readily interpreted using Gouterman's four orbital model.[19] Specifically, there are two principle $\pi-\pi^*$ transitions: a lower energy "Q-band" (~550−850 nm) and a higher energy "B-band" (~200−400 nm), arising from transitions from the highest occupied MO's (a_{1u} and a_{2u}) to the e_g LUMO. The reduced symmetry of the free-base porphyrazine splits the e_g LUMO and doubles the number of transitions. This change in symmetry is most easily observed in the Q-band region: symmetrical porphyrazines (e.g., metalated) exhibit *one* Q-band and unsymmetrical (e.g., free-base) *two* Q-bands. These dramatic changes will be used to analyze the behavior of the porphyrazines in this paper.

Metalation Studies. Metalation reactions were followed spectroscopically using samples of approximately 10^{-5} M $[H_2(Me\text{-}pyr)_8]^{8+}$ in aqueous buffer (2.0 M NaCl, 0.01 M phosphate, pH 4.00). The buffer simplified the observations by ensuring that the pyrrolic nitrogens were doubly protonated (vide infra); metalation was followed by UV−visible spectroscopy by monitoring the collapse of the two Q-bands of the free-base to the single Q-band that is indicative of metal insertion. The

(19) Gouterman, M. In *The Porphyrins*; Dolphin, D., Ed.; Academic Press: New York, 1978; Vol. III, pp 1−165.
(20) Jackson, A. H. In *The Porphyrins*; Dolphin, D., Ed.; Academic Press: New York, 1978; Vol. I, pp 365−388.
(21) Rosenthal, I.; Ben-Hur, E. In *Phthalocyanines: Properties and Applications*; Leznoff, C. C., Lever, A. B. P., Eds.; VCH Publishers: New York, 1989; Vol. 1, pp 393−425.
(22) Andersen, K.; Anderson, M.; Anderson, O. P.; Baum, S.; Baumann, T. F.; Beall, L. S.; Broderick, W. E.; Cook, A. S.; Eichhorn, D. M.; Goldberg, D.; Hope, H.; Jarrell, W.; Lange, S. J.; McCubbin, Q. J.; Mani, N. S.; Miller, T.; Montalban, A. G.; Rodriguez-Morgade, M. S.; Lee, S.; Nie, H.; Olmstead, M. M.; Sabat, M.; Sibert, J. W.; Stern, C.; White, A. J. P.; Williams, D. B. G.; Williams, D. J.; Barrett, A. G. M.; Hoffman, B. M. *J. Heterocycl. Chem.* **1998**, *35*, 1013−1042.
(23) Cook, A. S.; Williams, D. B. G.; White, A. J. P.; Williams, D. J.; Lange, S. J.; Barrett, A. G. M.; Hoffman, B. M. *Angew. Chem., Int. Ed. Engl.* **1997**, *36*, 760−761.
(24) Forsyth, T. P.; Williams, D. B. G.; Montalban, A. G.; Stern, C. L.; Barrett, A. G. M.; Hoffman, B. M. *J. Org. Chem.* **1998**, *63*, 331−336.
(25) Velazquez, C. S.; Broderick, W. E.; Sabat, M.; Barrett, A. G. M.; Hoffman, B. M. *J. Am. Chem. Soc.* **1990**, *112*, 7408−7410.
(26) (a) Linstead, R. P.; Noble, E. G.; Wright, J. M. *J. Chem. Soc.* **1937**, 911−921. (b) Hanack, M.; Thies, R. *Chem. Ber.* **1988**, *121*, 1225−1230. (c) Wöhrle, D.; Iskander, N.; Graschew, G.; Sinn, H.; Friedrich, E. A.; Maier-Borst, W.; Stern, J.; Schlag, P. *Photochem. Photobiol.* **1990**, *51*, 351−356. (d) Kudrevich, S. V.; van Lier, J. E. *Coord. Chem. Rev.* **1996**, *156*, 163−182.
(27) Leznoff, C. C. In *Phthalocyanines: Properties and Applications*; Leznoff, C. C., Lever, A. B. P., Eds.; VCH Publishers: New York, 1989; Vol. 1, pp 2−54.
(28) Fernández, D. A.; Awruch, J.; Dicelio, L. E. *J. Photochem. Photobiol. B* **1997**, *41*, 227−232.
(29) Wagner, J. R.; Ali, H.; Langlois, R.; Brasseur, N.; van Lier, J. E. *Photochem. Photobiol.* **1987**, *45*, 587−594.
(30) Stillman, M. J.; Nyokong, T. In *Phthalocyanines: Properties and Applications*; Leznoff, C. C., Lever, A. B. P., Eds.; VCH Publishers: New York, 1989; Vol. 1, pp 133−290.
(31) Smith, K. M. *Porphyrins and Metalloporphyrins*; Elsevier Scientific Publishing Co.: New York, 1975; pp 11−15, 234−238.
(32) Hambright, P.; Fleischer, E. B. *Inorg. Chem.* **1970**, *9*, 1757−1761.
(33) Stuzhin, P. A.; Khelevina, O. g. G.; Berezin, B. D. In *Phthalocyanines: Properties and Applications*; Leznoff, C. C., Lever, A. B. P., Eds.; VCH Publishers: New York, 1996; Vol. 4, pp 19−78.
(34) Kobayashi, N.; Fujihira, M.; Osa, T.; Kuwana, T. *Bull. Chem. Soc. Jpn.* **1980**, *53*, 2195−2200.

metal salts (typically chloride salts) were dissolved in the buffer before addition to the sample. Two metal complexes ($[Nipz(Me\text{-}pyr)_8]^{8+}$ and $[Cupz(Me\text{-}pyr)_8]^{8+}$) were prepared on a larger scale (~150 mg) for complete characterization and for use in aggregation studies.

pH Titrations. The pK_a values for the pyrrolic nitrogens of porphyrazine $[H_2pz(Me\text{-}pyr)_8]^{8+}$ in water were determined by UV−visible pH titrations. For a typical titration, 100 mL of 1.0×10^{-5} M porphyrazine at the appropriate ionic strength was prepared by dilution of a stock solution (10^{-3} M in porphyrazine). The pH of this solution was adjusted in increments of 0.1−0.2 pH units by addition of 5−300 μL portions of titrant (HCl or NaOH) with continuous stirring and pH monitoring. This solution also contained a dilute buffer (0.01 M phosphate) to keep the pH stable during the stages of the titration. For all titrations, the total amount of titrant added was less than 5% of the total volume and dilution corrections were unnecessary. Because the porphyrazine in basic solutions of low ionic strength is not stable for more than 5−10 min, the titrations were performed at ionic strengths of 0.1 M (NaCl) or higher. Under these conditions, the porphyrazine was completely stable over the range $1 \leq pH \leq 11$ during the time required for any titration experiment. As a precaution, 0.1 M NaCl titrations were begun at low pH; at 2.0 M, the results obtained were shown to be independent of titration direction.

Synthesis. 2,3-Bis(4-pyridyl)-2,3-dicyanomaleonitrile (1). A slurry of 4-pyridylacetonitrile hydrochloride (12.36 g, 80 mmol) and iodine (37.24 g, 147 mmol) in 1:1 Et_2O−MeOH (80 mL) was allowed to reflux under nitrogen for 1 h. The solution was cooled to room temperature, and 3 equiv of a 2.0 M NaOMe methanolic solution was added dropwise over 30 min. The reaction mixture was then refluxed for another 3 h, during which time a precipitate formed. The solution was filtered at room temperature and the solid washed with chilled MeOH−Et_2O (2:3, 500 mL). Elemental analysis of the precipitated solid indicated that **1** coprecipitates with 2 molecules of NaI. Recrystallization from hot $CHCl_3$ layered with Et_2O provided 3.40 g (37% yield) of white needles which were shown by elemental analysis to be free of NaI. ^{1}H NMR (DMSO-d_6): δ 8.87 (d, 1H), 7.85 (d, 1H). FAB$^+$-MS: *m*/*e* 233 ($M + H^+$). Anal. Found (calcd for $C_{14}H_8N_4$): C, 72.38 (72.40); H, 3.36 (3.47); N, 24.21 (24.12).

(2,3,7,8,12,13,17,18-Octakis(4-pyridyl)porphyrazinato)magnesium(II), [Mgpz(pyr)$_8$]. Magnesium metal (70 mg, 2.9 mmol) was added to 1-butanol (28 mL) and heated to reflux, at which time a small chip of iodine was added to initiate the formation of $Mg(OBu)_2$. Heating was continued for 12 h, over which time a white suspension of $Mg(OBu)_2$ formed. The solution was then cooled to room temperature, **1** (2.0 g, 8.0 mmol) was added, and the heating was continued at 100 °C. Initially, the reaction mixture turned light yellow upon dissolution of **1**, but within 15 min was a deep blue color. After 8 h, the solvent was removed by distillation and the solid washed with $CHCl_3$ (500 mL) to give a blue-black residue. The crude macrocycle was chromatographed twice over neutral alumina: the first column was eluted with 20% MeOH in $CHCl_3$, and the second with a gradient of 5% MeOH in $CHCl_3$ to 30% MeOH in $CHCl_3$. Teal-blue solid [Mgpz(pyr)$_8$] was obtained in 20% yield (418 mg). Poor solubility in organic solvents made the material difficult to characterize, and dissolution in acidic solvents was associated with concomitant loss of Mg^{2+} from the core. UV−vis (20% MeOH in $CHCl_3$): λ_{max} (ϵ, $mM^{-1}\ cm^{-1}$) 376 (99), 634 (125). Emission (20% MeOH in $CHCl_3$): λ_{max} (excitation λ) 645 (394). ^{1}H NMR (pyridine-d_5): δ 9.14 (d, 1H), 8.33 (d, 1H). FAB$^+$-MS: *m*/*e* 954 ($M + 2H^+$). Anal. Found (calcd for $C_{56}H_{32}N_{16}Mg\cdot 2H_2O$): C, 67.47 (67.99); H, 3.85 (3.67); N, 22.15 (22.65).

2,3,7,8,12,13,17,18-Octakis(4-pyridyl)porphyrazine, [H$_2$pz(pyr)$_8$]. Macrocycle [Mgpz(pyr)$_8$] was dissolved in aqueous HCl (10 mL of concentrated HCl in 100 mL of H_2O) and stirred for 1 h. The blue acidic solution was chilled with ice, made basic with NH_4OH, and centrifuged at 10 °C and 3100 rpm for 3 h. The supernatant was decanted and the green crude product was chromatographed on alumina with 10% MeOH in $CHCl_3$ to give approximately 90% yield of [H$_2$pz(pyr)$_8$]. UV−vis (20% MeOH in $CHCl_3$): λ_{max} (ϵ, $mM^{-1}\ cm^{-1}$) 366 (68), 590 (43), 658 (66). Emission (20% MeOH in $CHCl_3$): λ_{max} (excitation λ) 669 (450). ^{1}H NMR (20% DCl in D_2O): δ 10.46 (d, 1H), 10.21 (d, 1H). FAB$^+$-MS: *m*/*e* 932 ($M + 2H^+$).

2,3,7,8,12,13,17,18-Octakis(*N*-methyl-4-pyridiniumyl)porphyrazine, [H$_2$pz(Me-pyr)$_8$]$^{8+}$. Porphyrazine [H$_2$pz(pyr)$_8$] (495 mg, 0.53 mmol) was dissolved in DMF (45 mL) by heating for 30 min at 80 °C after which a 100-fold excess of methyl 4-toluenesulfonate (8.0 mL, 9.9 g, 53 mmol) was added. Heating continued at 100 °C for 3 days, over which time the blue solution became green with a metallic blue precipitate. ^{1}H NMR could be used to monitor the progress of the alkylation reaction since incomplete methylation lowers the macrocycle's symmetry and increases the number of pyridyl-proton doublets and *N*-methyl proton signals. The reaction mixture was stored at 0 °C overnight and the solid filtered over Celite. The crude [H$_2$pz(Me-pyr)$_8$](tos)$_8$ was dissolved in H_2O (600 mL, pH ≈ 6) and was washed with 4 × 250 mL portions of CH_2Cl_2. A saturated solution of tetrabutylammonium hexafluorophosphate ((TBA)PF_6) in MeOH was added (10 mL) to form a green precipitate which was filtered out, washed with H_2O and MeOH, and dried under vacuum to give 65% yield (762 mg, 0.34 mmol) of [H$_2$pz(Me-pyr)$_8$](PF$_6$)$_8$. As the hexafluorophosphate salt, the compound was only slightly soluble in water. It was freely soluble in such solvents as CH_3CN, DMSO, and DMF and was readily recrystallized from slow vapor diffusion of acetone into CH_3CN for analytical measurements. Emission (DMSO): λ_{max} (excitation λ) 723 (680). Anal. Found (calcd for $C_{64}H_{58}N_{16}P_8F_{48}\cdot H_2O$): C, 34.86 (34.43); H, 3.41 (3.52); N, 9.69 (10.05). ^{1}H NMR (DMSO-d_6): δ 9.32 (d, 2H), 8.92 (d, 2H), 4.61 (s, 3H). To obtain the chloride salt, [H$_2$pz(Me-pyr)$_8$](PF$_6$)$_8$ was stirred in water containing equilibrated Amberlite IRA-400(Cl) ion-exchange resin until all solid was dissolved to give a green solution (≈1 h). The solution was poured off of the resin, fresh resin added, and the solution stirred for an additional 1 h. Filtration and lyophilization of the solution gave dark green solid [H$_2$pz(Me-pyr)$_8$](Cl)$_8$ in approximately quantitative yield. As the chloride salt, the porphyrazine is freely soluble in water. UV−vis (2.0 M NaCl water buffered with 0.01 M phosphate, pH 4.00): λ_{max} (ϵ, $mM^{-1}\ cm^{-1}$) 266 (45), 380 (62), 614 (40), 676 (55). Emission (water, pH = 2.0 or 7.0): λ_{max} (excitation λ) 692 (660). ^{1}H NMR (D_2O, pH ≈ 7): δ 8.95 (d, 2H), 8.71 (d, 2H), 4.48 (s, 3H).

(2,3,7,8,12,13,17,18-Octakis(*N*-methyl-4-pyridiniumyl)porphyrazinato)nickel(II), [Nipz(Me-pyr)$_8$]$^{8+}$. [H$_2$pz(Me-pyr)$_8$](Cl)$_8$ (150 mg, 0.07 mmol) was dissolved in 2.0 M NaCl (buffered with 0.01 M phosphate to pH 4.00) (10 mL) to give a green solution. A 10-fold excess of $Ni(OAc)_2\cdot 4H_2O$ (169 mg, 0.7 mmol), dissolved in 2.0 M NaCl (5 mL) was added and the mixture heated at 60 °C for 15 min or until completion as monitored by changes in the UV−visible spectrum. After cooling of the solution to room temperature, (TBA)PF_6 in MeOH was added to precipitate [Nipz(Me-pyr)$_8$](PF$_6$)$_8$ and the slurry was centrifuged for 2 h at 3100 rpm and 10 °C and filtered. The solid was washed with MeOH, and 156 mg (0.07 mmol, ≈quantitative) was recrystallized from slow vapor diffusion of acetone into CH_3CN to give 65 mg (first crop, 41% yield, 0.03 mmol) of a very small, blue, rhombic crystalline material. Anal. Found (calcd for $C_{64}H_{56}N_{16}NiP_8F_{48}$): C, 33.52 (33.90); H, 2.90 (2.49); N, 9.57 (9.88). ^{1}H NMR (DMSO-d_6): δ 9.35 (d, 2H), 8.86 (d, 2H), 4.62 (s, 3H). The PF_6 counterion of porphyrazine $[Nipz(Me\text{-}pyr)_8]^{8+}$ was exchanged as in the case of the free-base porphyrazine [H$_2$pz(Me-pyr)$_8$](PF$_6$)$_8$ to give [Nipz(Me-pyr)$_8$](Cl)$_8$. UV−vis (2.0 M NaCl water buffered with 0.01 M phosphate, pH 4.00): λ_{max} (ϵ, $mM^{-1}\ cm^{-1}$) 270 (38), 368 (62), 642 (72).

(2,3,7,8,12,13,17,18-Octakis(*N*-methyl-4-pyridiniumyl)porphyrazinato)copper(II) Hexafluorophosphate, [Cupz(Me-pyr)$_8$](PF$_6$)$_8$. The desired porphyrazine was prepared analogously to the $[Nipz(Me\text{-}pyr)_8]^{8+}$ but using $CuCl_2\cdot 2H_2O$ and stirring the solution overnight at room temperature. To remove all metal salts and impurities, the solid was repeatedly precipitated from water with methanolic (TBA)PF_6 and washed with MeOH and a small amount of water, and the anion was exchanged for Cl^- by stirring over IRA-400(Cl) ion-exchange resin, decanting from the old resin, and stirring over fresh resin to ensure complete exchange before repeating the precipitation. Anal. Found (calcd for $C_{64}H_{58}N_{16}CuP_8F_{48}$): C, 34.19 (33.83); H, 2.95 (2.48); N 9.63 (9.86). The PF_6 counterion of porphyrazine [Cupz(Me-pyr)$_8$](PF$_6$)$_8$ was exchanged as in the case of the free-base porphyrazine [H$_2$pz(Me-pyr)$_8$](PF$_6$)$_8$ to give [Cupz(Me-pyr)$_8$](Cl)$_8$. UV−vis (2.0 M NaCl water buffered with 0.01 M phosphate, pH 4.00): λ_{max} (ϵ, $mM^{-1}\ cm^{-1}$) 266

Scheme 1. Synthesis of Octapyridylporphyrazines and Octakis(methylpyridiniumyl)porphyrazines[a]

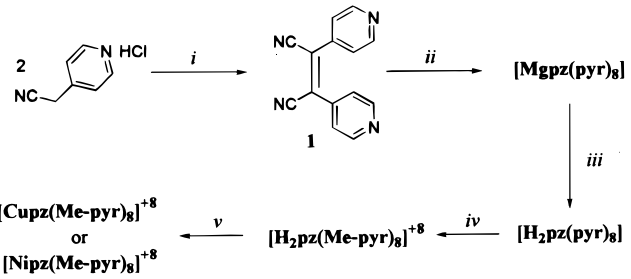

[a] Key: (*i*) 1:1 Et_2O−MeOH, I_2, NaOMe, reflux (37% yield); (*ii*) $Mg(O\text{-}nBu)_2$, n-BuOH, reflux (20% yield); (*iii*) dilute aqueous HCl; (*iv*) MeOTs, DMF, 3 days, 100 °C (65% yield); (*v*) MCl_2, 2.0 M NaCl, H_2O.

(55), 382 (62), 644 (100). EPR results: $g_{\|} = 2.16$, $A_{Cu} = 208$ G, $g_{\perp} = 2.06$, and $A_N = 17.8$ G.

Results

Octapyridylporphyrazines. Functionalized porphyrazines are typically synthesized by templated cyclization of the corresponding maleonitrile, as shown in Scheme 1. The published preparation of bis(2-pyridyl)maleonitrile[35] was adapted for the synthesis of bis(4-pyridyl)maleonitrile from the 4-pyridylacetonitrile hydrochloride salt (Scheme 1.*i*). Cyclization of the maleonitrile in refluxing Mg^{2+} butoxide[36] gave $[Mgpz(pyr)_8]$ (Scheme 1.*ii*). This compound is marginally soluble in most solvents, including chloroform, methanol, and pyridine, but a mixture of 20% MeOH in $CHCl_3$ provided sufficient solubility for extinction coefficient measurements and purification by alumina column chromatography. Demetalation in aqueous HCl (∼1.2 M) and precipitation by neutralization afforded the free-base macrocycle, $[H_2pz(pyr)_8]$ (Scheme 1.*iii*). This compound, which is more soluble in 20% MeOH/$CHCl_3$ than $[Mgpz(pyr)_8]$, likewise was chromatographically purified.

The optical spectrum of $[Mgpz(pyr)_8]$ (Figure 1A) exhibits a B-band (376 nm, 99 mM^{-1} cm^{-1}) and Q-band (634 nm, 125 mM^{-1} cm^{-1}) as well as the Q-band blue shoulder vibrational satellite typical of symmetrical, metalated porphyrazines. Excitation of $[Mgpz(pyr)_8]$ at 378 nm generates emission with a maximum at 650 nm (Figure 1A), with an excitation spectrum that corresponds to the UV−visible spectrum of $[Mgpz(pyr)_8]$ (data not shown). A list of the absorption and emission wavelengths for the new porphyrazines is presented in Table 1. Removal of Mg^{2+} and protonation of the core to form $[H_2pz(pyr)_8]$ gives the expected split Q-band with maxima at 590 nm ($\epsilon \sim 43$ mM^{-1} cm^{-1}) and 658 ($\epsilon \sim 66$ mM^{-1} cm^{-1}) (Figure 1B). The lower-energy λ_{max} consequently red-shifts the emission of $[H_2pz(pyr)_8]$ by 20 nm to 670 nm (Figure 1B). The excitation spectrum reflects the 2 Q-bands found in the UV−visible spectrum (data not shown).

As anticipated, both pyridylporphyrazines ($[Mgpz(pyr)_8]$ and $[H_2pz(pyr)_8]$) dissolve in aqueous HCl as the pyridyl nitrogens become protonated; however, optical spectra showed that even in dilute aqueous HCl (0.12 M), $[Mgpz(pyr)_8]$ undergoes demetalation to give $[H_2pz(pyr)_8]$. As a result, our studies focused on the acid−water solubility of only the free-base form, $[H_2pz(pyr)_8]$. Indeed, it was possible to generate the free-base form on a preparative scale by demetalating $[Mgpz(pyr)_8]$ with aqueous HCl and recovering the product by neutralization and precipitation from the water. The degree to which the peripheral pyridyl groups are protonated in aqeuous acid was not determined, but ^1H NMR of $[H_2pz(pyr)_8]$ in 20 wt % DCl in D_2O gave a symmetrical pyridyl proton resonance pattern (two doublets), consistent with the protonation of all the pyridyl nitrogens under these conditions.

$[H_2pz(H\text{-}pyr)_8]^{8+}$ in dilute aqueous HCl has the split Q-band typical of a free-base porphyrazine. The maximum wavelengths, however, are red-shifted 10−20 nm relative to the spectrum in 20% MeOH in $CHCl_3$; the B-band is shifted 10 nm to 376 nm, and the two Q-bands shift 18 and 16 nm to 608 and 674 nm, respectively (Figure 1C). $[H_2pz(H\text{-}pyr)_8]^{8+}$ in dilute aqueous HCl also has two bands at higher energy, at 258 and 290 nm. These higher-energy bands also can be seen in 20% MeOH in $CHCl_3$ solutions of $[Mgpz(pyr)_8]$ and $[H_2pz(pyr)_8]$; in this

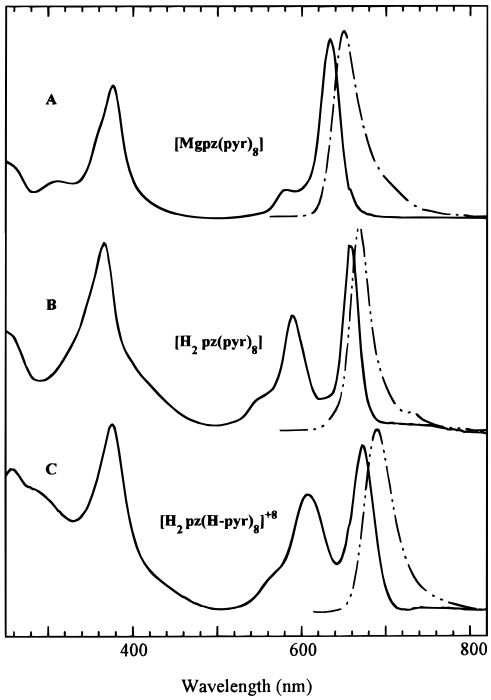

Figure 1. Absorption (—) and emission (— ·· —) of the octapyridylporphyrazines: (A) $[Mgpz(pyr)_8]$ in 20% MeOH in CHCl3, emission excitation at 378 nm; (B) $[H_2pz(pyr)_8]$ in 20% MeOH in CHCl3, emission excitation at 367 nm; (C) $[H_2pz(H\text{-}pyr)_8]^{8+}$ in aqueous HCl (∼1.2 M), emission excitation at 607 nm.

Table 1. Electronic Absorption Properties of Porphyrazines

compd[a]	UV−vis, nm (ϵ, mM^{-1} cm^{-1}) (B; Q)	emission, nm
$[Mgpz(pyr)_8]$ (a)	376 (99); 634 (125)	650
$[H_2pz(pyr)_8]$ (a)	366 (68); 590 (43), 658 (66)	670
$[H_2pz(pyr)_8]$ (b)	258, 290, 376; 608, 674	690
$[H_2pz(Me\text{-}pyr)_8]^{8+}$ (c)	380 (50); 680 (86)	723
$[H_2pz(Me\text{-}pyr)_8]^{8+}$ (d)	266, 380; 616, 678	696
$[H_2pz(Me\text{-}pyr)_8]^{8+}$ (e)	266 (45), 380 (62); 614 (40), 676 (55)	
$[H_1pz(Me\text{-}pyr)_8]^{7+}$ (f)	288, 332, 382; 672	686
$[pz(Me\text{-}pyr)_8]^{6+}$ (g)	287, 332, 385; 678	718
$[Nipz(Me\text{-}pyr)_8]^{8+}$ (e)	270 (38), 368 (62); 642 (72)	
$[Cupz(Me\text{-}pyr)_8]^{8+}$ (e)	266 (56), 322 (42), 382 (62); 644 (98)	

[a] Key: (a) 20% MeOH in $CHCl_3$; (b) dilute aqueous HCl; (c) DMSO; (d) H_2O pH 2.0, 2.0 M NaCl, 0.01 M phosphate; (e) H_2O pH 4.00, 2.0 M NaCl, 0.01 M phosphate; (f) H_2O pH 8.0, 2.0 M NaCl, 0.01 M phosphate; (g) H_2O pH 9.6, 2.0 M NaCl, 0.01 M phosphate.

(35) Piechucki, C.; Michalski, J. *Bull. Acad. Pol. Sci., Ser. Sci. Chim.* **1970**, *XVIII*, 605−607.
(36) Linstead, R. P.; Whalley, M. *J. Chem. Soc.* **1952**, 4839−4844.

Scheme 2

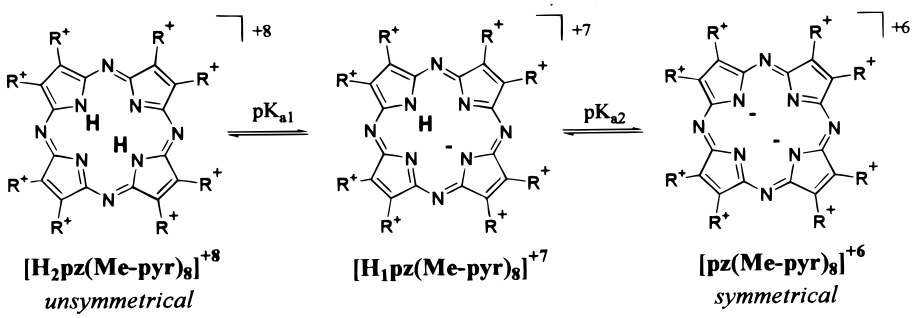

Table 2. Metalation Kinetics and Electronic Absorption Properties of [Mpz(Me-pyr)$_8$]$^{8+}$ [a]

metal (λ_{max}, nm)	relative rate[b]
Ba(II) (646); Ni(II) (642); Pd(II) (630)	+++
Co(II) (638)	++
Cu(II) (644); Cd(II)(674); Mn(III) (714); Zn(II) (660)	+

[a] Aqueous, with 2.0 M NaCl and 0.01 M phosphate at pH 4.00 buffer. [b] +++, overnight to several days; ++, 5−15 min; +, immediate formation of complex.

solvent system, the more energetic of the two bands is seen only as an end absorption. The second higher-energy band is observed at 312 nm for [Mgpz(pyr)$_8$] but appears to be buried underneath the B-band in [H$_2$pz(pyr)$_8$] (Figure 1B). The red-shifting of the overall spectrum for [H$_2$pz(H-pyr)$_8$]$^{8+}$ in aqueous acid versus that of [H$_2$pz(pyr)$_8$] in methanolic chloroform is reflected in a 20 nm shift in the emission to 690 nm (excitation, 607 nm) (Figure 1C), with an excitation spectrum similar to the optical spectrum (data not shown).

When a solution of [H$_2$pz(pyr)$_8$] in 20% MeOH in CHCl$_3$ is bubbled with HCl gas to generate [H$_2$pz(H-pyr)$_8$]$^{8+}$, its spectrum red-shifts, similar to the behavior in aqueous HCl, but the bands are greatly broadened, indicative of aggregation (spectrum not shown). The emission spectrum in acidic MeOH−CHCl$_3$ is similar to [H$_2$pz(H-pyr)$_8$]$^{8+}$ in dilute HCl in water, with emission at 690 nm (excitation at 607 nm), but the intensity is greatly reduced.

Octakis(methylpyridiniumyl)porphyrazines. Reaction of [H$_2$pz(pyr)$_8$] with an excess of methyl tosylate produced the octacationic octakis(*N*-methylpyridyl)porphyrazine, [H$_2$pz(Me-pyr)$_8$]$^{8+}$, which was recrystallized and characterized by ^{1}H NMR and elemental analysis (Scheme 1.*iv*). The simple spectrum, comprised of two sets of pyridyl doublets (δ = 8.95 and 8.71 ppm, 2 ^{1}H each) and a single methyl resonance (δ = 4.48 ppm, 3 ^{1}H), confirms the methylation of all eight pyridyl groups (Table 2).

Metalation of Octakis(methylpyridiniumyl)porphyrazine. To investigate the incorporation of metal ions by the free-base macrocycle, [H$_2$pz(Me-pyr)$_8$]$^{8+}$ in a high-salt/low-pH buffer (2.0 M NaCl, 0.01 M phosphate, pH 4.00) was treated with various metal salts (Ba(II), Cd(II), Co(II), Cu(II), Mn(III), Ni(II), Pd(II), and Zn(II)) at room temperature. In all cases, formation of the metal ion complex was indicated by the collapse of the two Q-bands of the free base UV−visible spectrum into the single Q-band spectrum of the metalated species. The λ_{max} for the Q-bands of various metalated octacationic porphyrazines are given in Table 2. Room-temperature reaction times varied; in the case of Cu(II), Cd(II), Mn(III), and Zn(II), the metalation proceeded immediately upon addition of the metal under the conditions employed. Co(II) took noticeably longer to complex with the porphyrazine; Ba(II), Ni(II), and Pd(II) yielded the metalated octakis(methylpyridiniumyl)porphyrazine after overnight reaction or heating.

The metalation reaction was repeated on a preparative scale to make [Nipz(Me-pyr)$_8$]$^{8+}$ and [Cupz(Me-pyr)$_8$]$^{8+}$ (Scheme 1.*v*.). The charged [Mpz(Me-pyr)$_8$]$^{8+}$ (M = "H$_2$", Ni, and Cu) porphyrazines were water soluble as the chloride salts but could be precipitated with tetrabutylammonium hexafluorophosphate and were purified by multiple cycles of redissolution and precipitation. Analytically pure samples were crystallized by slow vapor diffusion of acetone into an acetonitrile solution of the porphyrazine−PF$_6$ salt.

In 2.0 M NaCl, [Nipz(Me-pyr)$_8$]$^{8+}$ and [Cupz(Me-pyr)$_8$]$^{8+}$ exhibit UV−visible spectra very similar to that of [Mgpz(pyr)$_8$] (Table 1). The nickel porphyrazine has a B-band maximum of 368 nm (ϵ = 62 mM^{-1} cm^{-1}) and a single Q-band at 642 nm (ϵ = 72 mM^{-1} cm^{-1}). Higher energy absorption is observed as a broad band around 270 nm (ϵ = 38 mM^{-1} cm^{-1}). [Cupz(Me-pyr)$_8$]$^{8+}$ is similar with B- and Q- band absorptions at 382 nm (ϵ = 62 mM^{-1} cm^{-1}) and 644 nm (ϵ = 98 mM^{-1} cm^{-1}), respectively. In the case of [Cupz(Me-pyr)$_8$]$^{8+}$, however, the higher energy absorption is resolved into two peaks at 266 nm (ϵ = 56 mM^{-1} cm^{-1}) and 322 nm (ϵ = 42 mM^{-1} cm^{-1}). Both [Nipz(Me-pyr)$_8$]$^{8+}$ and [Cupz(Me-pyr)$_8$]$^{8+}$ possess a vibrational satellite on the blue side of the Q-band as seen in [Mgpz(pyr)$_8$]. As expected, no emission from [Nipz(Me-pyr)$_8$]$^{8+}$ or [Cupz(Me-pyr)$_8$]$^{8+}$ was observed due to quenching by the metal ions.

Optical and Acid−Base Properties of [H$_2$pz(Me-pyr)$_8$]$^{8+}$. The unmetalated octakis(methylpyridiniumyl)porphyrazine [H$_2$pz(Me-pyr)$_8$]$^{8+}$ in neutral water *did not* give the expected UV−visible spectrum with two Q-bands: only one Q-band was observed at 678 nm. A pattern containing two Q-bands, however, could be generated by addition of HCl to the solution. This dependence on pH indicates that the spectrum of "[H$_2$pz(Me-pyr)$_8$]$^{8+}$" in fact is responding to protonation/deprotonation of the pyrrolic nitrogens. The correlation between the Q-band pattern observed in the UV−visible spectrum and the degree of symmetry of the macrocycle can be used to make initial assignments of the species ([H$_x$pz(Me-pyr)$_8$]$^{n+}$, x = 0−4, n = 6−10) present at extremely acidic and extremely basic pH's.

Acidic Solution. The UV−visible spectrum of the species present at low pH (pH 1) has two Q-bands, limiting the possible species to [Hpz(Me-pyr)$_8$]$^{7+}$, [H$_2$pz(Me-pyr)$_8$]$^{8+}$, or [H$_3$pz(Me-pyr)$_8$]$^{9+}$. The presence of four protons or no protons in the core would give a symmetrical macrocycle with a single Q-band (Scheme 2), so x = 4 and x = 0 could be excluded. To distinguish between x = 1, 2, or 3 was not possible on the basis of the symmetry of the spectrum at pH 1; however, the fact that the additional charge created by three protons would be difficult to achieve on a macrocycle that was already +8 suggested that the species at pH 1 should be assigned as

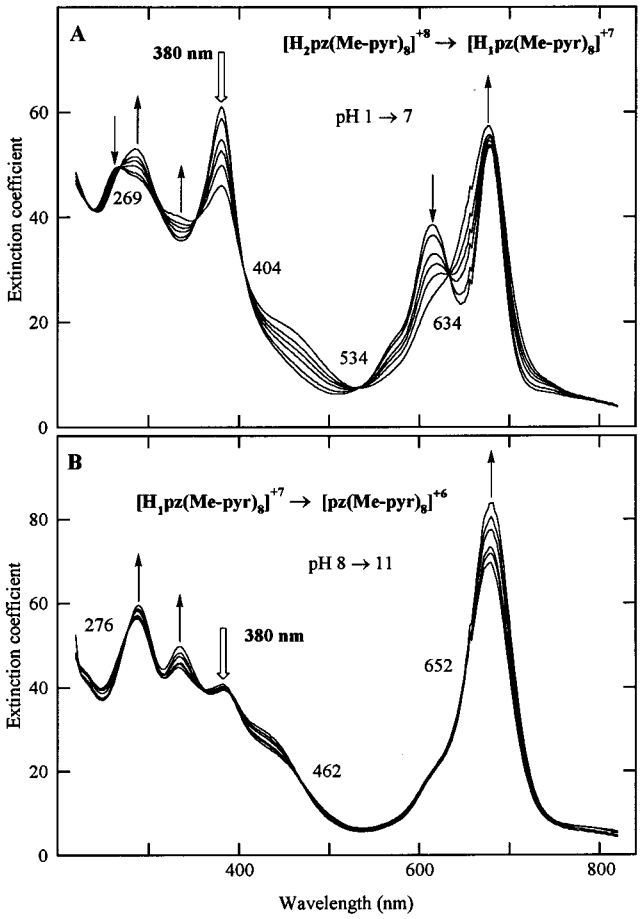

Figure 2. Selected spectra from the UV−visible titration of $[H_xpz(H\text{-}pyr)_8]^{8+}$ in 2.0 M NaCl and 0.01 M phosphate with NaOH. Arrows mark the increase or decrease in absorption as pH is increased; outlined arrows mark absorption at $\lambda = 380$ nm. (A) pH range from 1 to 7 showing the first set of isosbestic points at 269, 404, 534, and 634 nm for the first deprotonation of the pyrrolic nitrogens. (B) pH range from 8 to 11 showing the second set of isosbestic points 276, 462, and 652 nm for the second deprotonation.

$[H_2pz(Me\text{-}pyr)_8]^{8+}$. This assignment was supported by the fact that the tetrakis(*N*-methylpyridiniumyl)porphyrin (H_2TMPyP^{4+}), which is only tetracationic, does not acquire a third pyrrolic proton until pH 1.5.[32] Determination of the number of deprotonations occurring in the range of pH 1−11 and the assignment of the other species involved confirms $x = 2$ at pH 1 (see below).

Basic Solution. At high pH (pH 11), the $[H_xpz(Me\text{-}pyr)_8]^{n+}$ species present has a single Q-band. This pattern, of course, is compatible with $x = 0$; however, it is not known whether a porphyrazine with $x = 1$ is symmetrical (proton is shared by the four pyrrolic nitrogens) or unsymmetrical (proton is localized on one pyrrole nitrogen), so symmetry arguments cannot a priori rule out $x = 1$ (Scheme 2).

pH Titrations. pH titrations monitored by UV−visible spectroscopy were used to characterize the steps involved in going from pH 1 to pH 11. Example UV−visible spectra at various pH values are shown in Figure 2. Initial titrations were conducted at 2.0 M NaCl concentrations because $[H_xpz(Me\text{-}pyr)_8]^{n+}$ displays greater stability at high pH in solutions of high ionic strength (see Experimental Section, Methods).

Close examination of the spectra taken between pH 1 and pH 11 shows that there is no single set of isosbestic points, which indicates the occurrence of more than one deprotonation step. For solutions with 2.0 M NaCl, plots of the absorbance at various wavelengths versus pH show two inflection points over

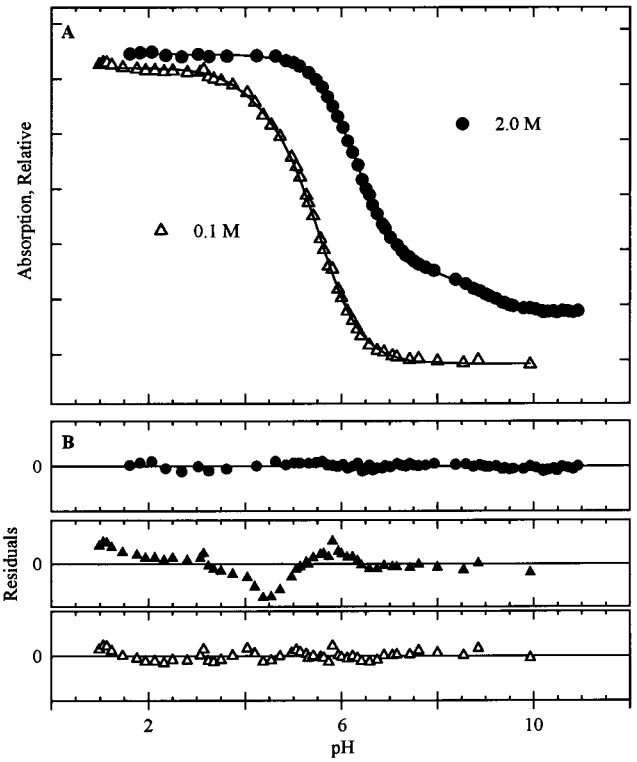

Figure 3. Results from the titration of $[H_xpz(H\text{-}pyr)_8]^{8+}$ in 2.0 M NaCl and 0.1 M NaCl with 0.01 M phosphate. (A) Absorption at $\lambda = 380$ nm for 0.1 M NaCl (△) and 2.0 M NaCl (●). Curve fit results are overlaid (−). (B) Difference between the fit and actual data, expanded to be twice the scale of the data in panel A: 2.0 M NaCl residuals (●), 0.1 M NaCl with fit for a single deprotonation (▲), and 0.1 M NaCl fit for two deprotonations (△).

the pH range 1−11, associated with two such steps (Figure 3). If the initial species is $x = 2$ (as above), then the final species at pH 11 must be $x = 0$ (Scheme 2). In fact, there are no other combinations of species to account for (i) two deprotonation steps, (ii) an unsymmetrical acidic species, and (iii) a symmetrical doubly deprotonated species Separation of the set of spectra into two pH ranges as shown in Figure 2 discloses the occurrence of separate sets of isosbestic points associated with the two different transitions. At low pH (Figure 2A), the isosbestic points at 269, 404, 534, and 634 nm are associated with the transition from $[H_2pz(Me\text{-}pyr)_8]^{8+}$ to $[Hpz(Me\text{-}pyr)_8]^{7+}$. At higher pH (Figure 2B), the transition from $[Hpz(Me\text{-}pyr)_8]^{7+}$ to $[pz(Me\text{-}pyr)_8]^{6+}$ is represented by isosbestic points at 276, 462, and 652 nm.

To extend the qualitative analysis of the pH titrations, UV−visible spectra (220−820 nm) were collected at intervals between pH 1 and 11; 70 intervals were employed for solutions with 2.0 M NaCl, and 53 intervals for 0.1 M NaCl. Titration profiles at 30 wavelengths were selected (profiles of absorbance vs pH were taken at approximately every 20 nm over the 220−820 nm range) and globally fit to a model involving two deprotonation steps. The measured absorbance at a given wavelength and pH, A_0, is the sum of the contributions from the species present:

$$A_0 = \epsilon_{H2}[H_2pz^{8+}] + \epsilon_{H1}[H_1pz^{7+}] + \epsilon_{pz}[pz^{6+}] \qquad (1)$$

Here ϵ_{H2}, ϵ_{H1}, and ϵ_{pz} are the extinction coefficients at that particular wavelength and $[H_2pz^{8+}]$, $[Hpz^{7+}]$, and $[pz^{6+}]$ are the concentrations of $[H_2pz(Me\text{-}pyr)_8]^{8+}$, $[Hpz(Me\text{-}pyr)_8]^{7+}$, and

$[pz(Me\text{-}pyr)_8]^{6+}$, respectively. Mass balance gives

$$[total_{pz}] = [H_2pz^{8+}] + [Hpz^{7+}] + [pz^{6+}] \quad (2)$$

where $[total_{pz}]$ is the total concentration of porphyrazine. The deprotonation steps can be written as

$$H_2pz^{8+} \rightleftharpoons H^+ + Hpz^{7+} \quad K_1 = \frac{[H_1pz^{7+}][H^+]}{[H_2pz^{8+}]} \quad (3)$$

and

$$H_1pz^{7+} \rightleftharpoons H^+ + pz^{6+} \quad K_2 = \frac{[pz^{6+}][H^+]}{[Hpz^{7+}]} \quad (4)$$

Equations 2−4 can be solved for the pH-dependent concentrations of $[H_2pz(Me\text{-}pyr)_8]^{8+}$, $[Hpz(Me\text{-}pyr)_8]^{7+}$, and $[pz(Me\text{-}pyr)_8]^{6+}$ in terms of K_1, K_2, and $[total_{pz}]$ and substituted into eq 1 to give

$$A_0 = \epsilon_{H2}\frac{[total_{pz}][H^+]^2}{K_1K_2 + [H^+]^2 + K_1[H^+]} + \epsilon_{H1}\frac{[total_{pz}]K_1[H^+]}{K_1K_2 + [H^+]^2 + K_1[H^+]} + \epsilon_{pz}\left[[total_{pz}] - \frac{[total_{pz}]([H^+]^2 + K_1[H^+])}{K_1K_2 + [H^+]^2 + K_1[H^+]}\right] \quad (5)$$

Through use of this equation, the pH-dependent absorbance profiles at multiple wavelengths were fit to generate K_1, K_2, $\epsilon_{H2}(\lambda)$, $\epsilon_{H1}(\lambda)$, and $\epsilon_{pz}(\lambda)$. Iteration of the values was continued until deviation of the residuals from zero was less than the precision of the UV−visible measurements. A typical fit is overlaid on the data in Figure 3, with the residuals from the fitting (expanded) shown in panel 3B. The acid dissociation constants for the pyrrolic nitrogens of $[H_2pz(Me\text{-}pyr)_8]^{8+}$ in 2.0 M NaCl were determined to be $pK_1 = 6.3$ and $pK_2 = 8.8$.

A similar approach was taken for titrations at 0.1 M NaCl. Plots of absorbance at various wavelengths versus pH *appeared* to possess only one inflection point at low ionic strength, seemingly indicating that either only one deprotonation was occurring or that the two deprotonations were simultaneous (Figure 3). However, attempts to fit the curves with a single-deprotonation model yielded unacceptably large, systematic deviations in the residuals (Figure 3B). A fit to a double deprotonation with $pK_1 = pK_2$ was even worse. An inflection point around pH 5 in the residuals suggested that data represent two sequential deprotonations as in 2.0 M NaCl but with pK_a values that are more similar. Iterative fitting with the two-deprotonation model (see above) gave acceptable residuals (Figure 3B) with $pK_1 = 4.1$ and $pK_2 = 5.6$.

The resulting two-deprotonation model was used to calculate the pH-dependent concentration profiles of the three species involved (Figure 4). The shift in the deprotonation process to higher pH with increasing ionic strength is apparent, as is a broadening in the range over which the two steps occur. This is most easily discussed in terms of the intermediate, singly deprotonated species $[Hpz(Me\text{-}pyr)_8]^{7+}$. At low ionic strength (0.1 M NaCl), this species is present in greatest concentration (72%) at pH 4.7, with appreciable amounts of both $[H_2pz(Me\text{-}pyr)_8]^{8+}$ (17%) and $[pz(Me\text{-}pyr)_8]^{6+}$ (10%). By 2.0 M ionic strength the maximum concentration of $[Hpz(Me\text{-}pyr)_8]^{7+}$ is

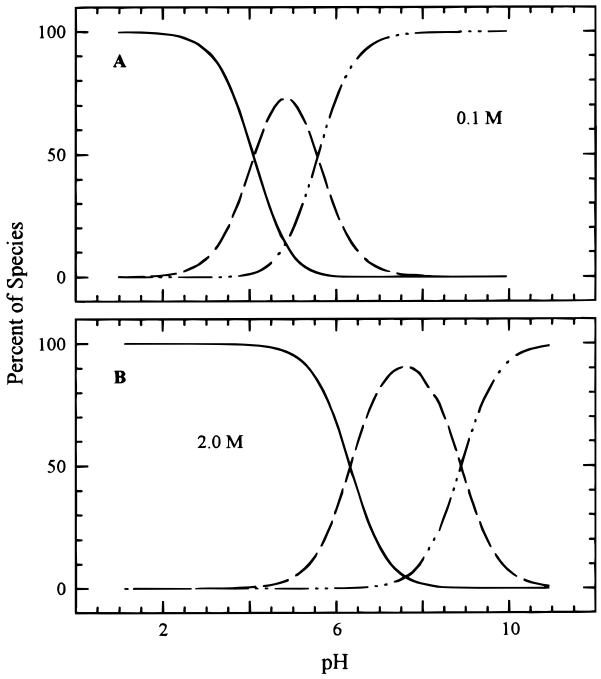

Figure 4. Percentage of species present in solution versus pH: $[H_2pz(H\text{-}pyr)_8]^{8+}$ (—); $[Hpz(H\text{-}pyr)_8]^{7+}$ (— —); $[pz(H\text{-}pyr)_8]^{6+}$ (— •• —). Panel A: 0.1 M NaCl. Panel B: 2.0 M NaCl.

90% and appears at pH 7.6. These ionic-strength variations reflect changes in the difference between the pK_a's for the first and second deprotonation (ΔpK_a); at high ionic strength $\Delta pK_a = 2.5$ and the deprotonations are almost sequential, whereas at low ionic strength $\Delta pK_a = 1.5$ and the deprotonations are more substantially overlapped. Indeed, the two-step deprotonation at low ionic strength was difficult to observe because of the smaller ΔpK_a and the lesser accumulation of the intermediate species. The ionic strength dependence of the two sets of pK_a's is discussed below.

In addition to determining the pK_a values, the fitting of the UV−visible spectra versus pH yields the extinction coefficients at multiple wavelengths and, hence, the optical spectra of $[H_x\text{-}pz(Me\text{-}pyr)_8]^{n+}$ ($x = 0$, 1, and 2 with $n = 6$, 7, and 8, respectively). Figure 5 shows plots of the calculated extinction coefficients vs wavelength for the three species at 2.0 M NaCl with comparison to the experimental spectra for $[H_2pz(Me\text{-}pyr)_8]^{8+}$ and $[pz(Me\text{-}pyr)_8]^{6+}$ at pH 1 and pH 11, respectively. For these two species, the calculated and the experimental spectra are identical; even the blue vibrational shoulder on the Q-bands is reproducible. The calculation also gives the optical spectrum of $[Hpz(Me\text{-}pyr)_8]^{7+}$, which cannot be obtained directly because it does not exist without appreciable equilibrium amounts of $[H_2pz(Me\text{-}pyr)_8]^{8+}$ and $[Hpz(Me\text{-}pyr)_8]^{7+}$. Interestingly, the spectrum of intermediate $[Hpz(Me\text{-}pyr)_8]^{7+}$ has a single but broadened Q-band. This suggests that the $[Hpz(Me\text{-}pyr)_8]^{7+}$ macrocycle may be essentially symmetrical, with the single proton in the core centered between the pyrrolic nitrogens.

Luminescence. As previously mentioned, the $[Nipz(Me\text{-}pyr)_8]^{8+}$ and $[Cupz(Me\text{-}pyr)_8]^{8+}$ porphyrazine emission is quenched by the presence of the metal ion. All three protonation states of the metal-free macrocycle, however, display strong fluorescence (Figure 5). The fluorescence of the diprotonated $[H_2pz(Me\text{-}pyr)_8]^{8+}$ was collected at pH 2.0 and 2.0 M NaCl, where it is present in approximately 100%; that of $[Hpz(Me\text{-}pyr)_8]^{7+}$ is approximated by the emission of a solution at pH 8.0, with 2.0 M NaCl, where $[Hpz(Me\text{-}pyr)_8]^{7+}$ is present in

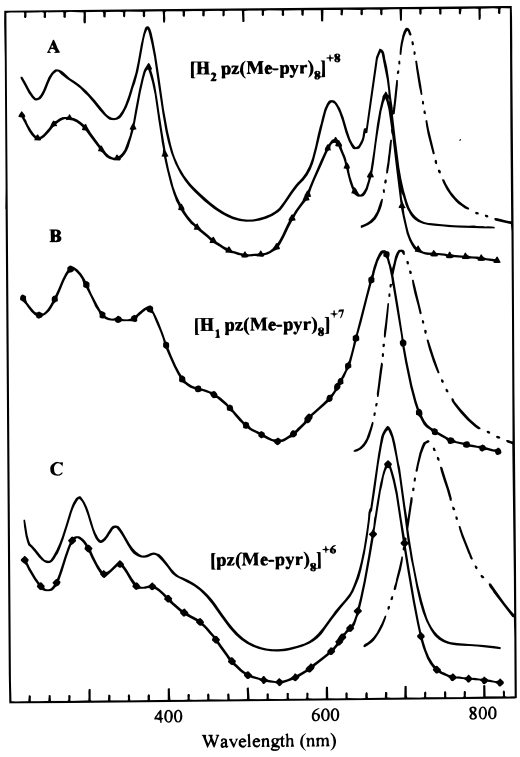

Figure 5. Comparison of the actual UV−visible spectra of $[H_2pz(H\text{-}pyr)_8]^{8+}$ (—, panel A) and $[pz(H\text{-}pyr)_8]^{6+}$ (—, panel C) to the calculated UV−visible spectra of $[H_2pz(H\text{-}pyr)_8]^{8+}$ (— —, panel A), $[Hpz(H\text{-}pyr)_8]^{7+}$ (—•—, panel B), and $[pz(H\text{-}pyr)_8]^{6+}$ (— ◆ —, panel C). Lines used to connect the calculated extinction coefficients have been smoothed to guide the eye. Emission (—••—) is at pH 2.0 (panel A), pH 8.0 (panel B), and pH 9.6 (panel C), in which the majority of porphyrazine is in the form $[H_2pz(H\text{-}pyr)_8]^{8+}$, $[Hpz(H\text{-}pyr)_8]^{7+}$, and $[pz(H\text{-}pyr)_8]^{6+}$, respectively. All solutions contain 2.0 M NaCl and 0.01 M phosphate.

88%; and that of $[pz(Me\text{-}pyr)_8]^{6+}$ is approximated by the emission at pH 9.6, 2 M NaCl, where it is present to is 83%. Excitation spectra confirmed that the emissive species in solution are the intended forms of $[H_xpz(Me\text{-}pyr)_8]^{n+}$ ($x = 0$, 1, and 2 with $n = 6$, 7, and 8, respectively).[37] Figure 5 shows that the longest-wavelength emission of all three protonated forms a maximum ~ 690 nm: emission from the diprotonated state is maximum at 696 nm (Table 1), and that from the monoprotonated form is at 686 nm, while that from the deprotonated species is red-shifted to 718 nm.

Aggregation. Aggregation of charged porphyrinic macrocycles in aqueous solution has been a topic of much controversy.[38−40] We observed a very broad, weak band around 760 nm in the UV−visible spectra of the cationic porphyrazines $[H_2pz(Me\text{-}pyr)_8]^{8+}$, $[Nipz(Me\text{-}pyr)_8]^{8+}$, and $[Cupz(Me\text{-}pyr)_8]^{8+}$ immediately upon dissolution, which disappeared over time to give the spectra discussed above. This band did not grow with increasing concentration of porphyrazine, indicating that it did not correspond to an equilibrium aggregation of the macrocycles; most likely it is due to slow dissolution of the solid material. Nonetheless, we used several different techniques to confirm the monomeric nature of our octacationic porphyrazines. In aqueous solutions (2.0 M NaCl, 0.01 M phosphate, pH 4.00) the porphyrazines $[H_2pz(Me\text{-}pyr)_8]^{8+}$, $[Nipz(Me\text{-}pyr)_8]^{8+}$, and $[Cupz(Me\text{-}pyr)_8]^{8+}$ exhibit linear plots of aborbance vs concentration over the range 1×10^{-7}−~4×10^{-5} M and there is no apparent broadening of the spectra or hypochromicity as concentration increases. Also, we see emission from the $[H_2pz(Me\text{-}pyr)_8]^{8+}$, which would in general be quenched by aggregation. Finally, the EPR spectrum of $[Cupz(Me\text{-}pyr)_8]^{8+}$ in frozen glass was taken because dimers of copper tetraazaporphyrins have well-defined EPR spectra[41−43] and dimerization is favored by cooling of the solution. Concentrations as high as 10^{-3} M in $[Cupz(Me\text{-}pyr)_8]^{8+}$ at 77 K gave a pattern indicative of a monomeric species. We therefore conclude that $[Cupz(Me\text{-}pyr)_8]^{8+}$ is monomeric in solution at room temperature and that the same is true for $[H_2pz(Me\text{-}pyr)_8]^{8+}$ and $[Nipz(Me\text{-}pyr)_8]^{8+}$.

Discussion

We have prepared the porphyrazines $[Mpz(pyr)_8]$ (M = Mg and "H_2") and $[Mpz(Me\text{-}pyr)_8]^{8+}$ (where M = "H_2", Ba(II), Cd(II), Co(II), Cu(II), Mn(III), Ni(II), Pd(II), and Zn(II)). The octakis(methylpyridiniumyl)porphyrazines are soluble in water, and the acid/base equilibria of the internal pyrrole protons were determined for $[H_2pz(Me\text{-}pyr)_8]^{8+}$. Two deprotonation steps were observed over the pH range of 1−11, corresponding to the transitions from $[H_2pz(Me\text{-}pyr)_8]^{8+}$ to $[Hpz(Me\text{-}pyr)_8]^{7+}$ (pK_{a1}) and from $[Hpz(Me\text{-}pyr)_8]^{7+}$ to $[pz(Me\text{-}pyr)_8]^{6+}$ (pK_{a2}). At 0.1 M ionic strength, the two pK_a values are 4.1 and 5.6, respectively; to our knowledge, these are the lowest values yet observed for a porphyrin or phthalocyanine in aqueous solution.[13,31−33] At 2.0 M ionic strength the acidity of the pyrrole protons is lessened and the pK_a values shift to 6.3 and 8.8. The closest related porphyrin for which the acidity of the pyrrole protons has been measured in aqueous media is the tetrakis(*N*-methylpyridiniumyl)porphyrin, H_2TMPyP^{4+}, whose first deprotonation step (H_2TMPyP^{4+} to $HTMPyP^{3+}$) is reported to occur with a pK_a of 12.9 at 0.1 M ionic strength and lower.[32] Thus, the octakis(methylpyridiniumyl)porphyrazine is more acidic than H_2TMPyP^{4+} by ~ 9 pK_a units!

Two major factors contribute to the extremely low pK_a's reported here. The first is the *meso*-nitrogen substitution in the porphyrazine. Sheinin et al. have shown that the electron-withdrawing *meso*-nitrogens help to stabilize the negative charge on a deprotonated pyrrolic nitrogen of a porphyrazine and thereby greatly increase their acidity as compared to an otherwise identical porphyrin.[33,44]

The second contribution to the increased acidity of $[H_2pz(Me\text{-}pyr)_8]^{8+}$, the electrostatic stabilization of the basic (anionic) form of the pyrroles by the positive charges of the *N*-methylpyridiniumyl moieties, varies with solution conditions. As the ionic strength is increased, the favorable electrostatic interaction between the anionic porphyrazine core and the peripheral cationic pyridinium groups is progressively "shielded" by the mobile ions in the solution, tending to *lower* the acidity

(37) Furthermore, the emission is solvent-dependent: $[H_2pz(pyrMe\text{-}pyr)_8]^{8+}(PF_6)_8$ dissolves in DMSO to give a green solution which is stable under a nitrogen atmosphere. The absorption spectrum contains a single Q-band at 678 nm (indicative of deprotonation of the pyrrolic nitrogens; see above), and upon excitation at 660 nm, displays a strong emission at 723 nm.

(38) Kano, K.; Takei, M.; Hasimoto, S. *J. Phys. Chem.* **1990**, *94*, 2181−2187.
(39) Pasternack, R. F.; Huber, P. R.; Boyd, P.; Engasser, G.; Francesconi, L.; Gibbs, E.; Fasella, P.; Venturo, G. C.; Hinds, L. d. *J. Am. Chem. Soc.* **1972**, *94*, 4511−4517.
(40) Dixon, D. W.; Steullet, V. *J. Inorg. Biochem.* **1998**, *69*, 25−32.
(41) Belford, R. L.; Chasteen, N. D.; So, H.; Tapscott, R. E. *J. Am. Chem. Soc.* **1969**, *91*, 4675−4680.
(42) Collman, J. P.; Elliott, C. M.; Hulbert, T. R.; Tovrog, B. S. *Proc. Natl. Acad. Sci. U.S.A.* **1977**, *74*, 18−22.
(43) Schramm, C. J.; Hoffman, B. M. *Inorg. Chem.* **1980**, *19*, 383−385.
(44) Sheinin, V. B.; Berezin, B. D.; Khelevina, O. G.; Stuzhin, P. A.; Telegin, F. Y. *Zh. Org. Khim.* **1985**, *21*, 1571−1576.

(increase pK_a) with increasing ionic strength. However, this effect is diminished by a competing one: an increase in ionic strength simultaneously tends to *raise* the acidity (decrease pK_a) by reducing the "charging" free energy required to create the negative charge(s) on the pyrroles.

To heuristically examine the competition between the two ionic-strength effects, one can consider the low-ionic-strength limit of the Debye−Hückel model[45,46] (which most definitely does *not* actually apply quantitatively in our experiments!). The ionic-strength dependent contribution to the pyrrolic pK_a from $n = 8$ peripheral positive charges is the same for both deprotonation steps of $[H_2pz(Me\text{-}pyr)_8]^{8+}$ (provided that the distribution of anionic charge is the same in the singly and doubly deprotonated macrocycle); it is proportional to $[+8\sqrt{C}]$, where the ionic strength equals the concentration of NaCl (C). The competing contribution from the charging free energy associated with the loss of the "pth" proton from the pyrrolic nitrogens ($p = 1$ for the first, $p = 2$ for the second) is proportional to the difference in the *square* of the charge on the basic and acidic forms, $[-\sqrt{C}(2p - 1)]$, and thus will be larger for the second deprotonation step where the core charge goes from −1 to −2. Overall, the ionic-strength dependent contribution to the pK_a (δpK_a) for the loss of the "pth" proton should therefore go roughly as $\delta pK_a \sim \sqrt{C}[8 - (2p - 1)]$.

According to this formula, as the ionic strength is raised, the screening of the attractive interactions with the eight pyridinium charges should dominate, and the pK_a values should increase with increasing [NaCl], as observed. Note that reducing the number of peripheral positive charges will change the balance between the two effects; in fact, over a similar change in ionic strength (0.2 to 2.0 M $NaNO_3$), the pK_a's for the monoacid and diacid of $TMPyP^{4+}$ change by only 0.8 (pK_a of 1.4 to 2.2) and ~0.2 (presuming a pK_a of 0.9 to ~0.7), respectively.[47] However, the formula also predicts that the change in pK_{a2} caused by an increase in [NaCl] should be less than the change in pK_{a1}, which is contrary to the observation that an increase from 0.1 to 2.0 M ionic strength raises pK_{a1} ($p = 1$) by 2.2 units but raises pK_{a2} ($p = 2$) by 3.2 units. This could mean that the location of the charges on the macrocycle pyrroles is *not* the same for the $[Hpz(Me\text{-}pyr)_8]^{7+}$ and $[pz(Me\text{-}pyr)_8]^{6+}$, and that there is differential delocalization of the charges over the ring in these two states.[48]

Generally, the preparative incorporation of metal ions into porphyrinic macrocycles employs rather strenuous conditions (e.g., heating in DMF).[31,49] However, the rate of metalation for H_2TMPyP^{4+} typically is high at room temperature despite the repulsion between the cationic periphery and the cationic metal.[1,32,50,51] We find that $[H_2pz(Me\text{-}pyr)_8]^{8+}$ behaves similarly, rapidly incorporating a variety of metal ions at room temperature. Presumably, the increased acidity of the pyrrolic nitrogens and ionic shielding of the cationic periphery more than compensate for the repulsion of the cationic transition metal ion to the porphyrazine periphery. The metal dependence of the rates of incorporation appear to be similar for $TMPyP^{4+}$ and $[H_2pz(Me\text{-}pyr)_8]^{8+}$; for example, both macrocycles immediately incorporate Cu(II) but require longer times and heating to incorporate Ni(II). The Cu(II) and Ni(II) complexes $[Cupz(Me\text{-}pyr)_8]^{8+}$ and $[Nipz(Me\text{-}pyr)_8]^{8+}$ have been synthesized on a preparative scale and characterized. Further studies will investigate more closely the rates of metal ion incorporation and the properties of other metallo−octaplus porphyrazines.

In conclusion, we have reported the synthesis and characterization of octapyridylporphyrazines and their octacationic derivatives $[Mpz(Me\text{-}pyr)_8]^{8+}$, M = "$H_2$", Cu, and Ni. By extension from the keen interest in the pyridyl porphyrins it can be assumed that the new macrocycles will have many applications. For example, the interactions of tetracationic $MTMPyP^{4+}$ with DNA have been studied intensively,[2,52−54] and we find that $[Hpz(Me\text{-}pyr)_8]^{7+}$ binds strongly to calf thymus DNA.[55] In addition, dipyridylmaleonitrile (**1**) can be cocyclized with various other dinitriles that have been developed in our laboratory[22−25] to produce pyridylporphyrazines with a wide range of potential applications.

Acknowledgment. This work was supported by the National Science Foundation (Grant CHE-9727590), by a fellowship from the United States Army (USAMRMC Grant No. DAMD17-94-J-4466), and by a travel grant from NATO.

IC990410S

(45) Edsall, J. T.; Wyman, J. *Biophysical Chemistry*, 1st ed.; Academic Press Inc.: New York, 1958; Vol. 1, pp 241−322.
(46) Castellan, G. W. *Physical Chemistry*, 3rd ed.; Benjamin/Cummings Publishing Co., Inc.: Reading, MA, 1983; pp 358−367.
(47) Baker, H.; Hambright, P.; Wagner, L. *J. Am. Chem. Soc.* **1973**, *95*, 5942−5946.
(48) Titrations of cationic porphyrins have been shown to depend on the identity of the counterion present;[47] thus, titration experiments using different salts will be necessary to determine whether, for example, the sodium ions may ion pair with the deprotonated pyrrolic nitrogens, thereby enhancing the acidity of the porphyrazine.
(49) Buchler, J. W. In *The Porphyrins*; Dolphin, D., Ed.; Academic Press: New York, 1978; Vol. I, pp 389−483.
(50) Choi, E. I.; Fleischer, E. B. *Inorg. Chem.* **1963**, *2*, 94−97.
(51) Fleischer, E. B.; Choi, E. I.; Hambright, P.; Stone, A. *Inorg. Chem.* **1964**, *3*, 1284−1287.
(52) Carvlin, M. J.; Fiel, R. J. *Nucleic Acids Res.* **1983**, *11*, 6121−6139.
(53) Marzilli, L. G. *New J. Chem.* **1990**, *14*, 409−420.
(54) Pasternack, R. F.; Gibbs, E. J. *Met. Ions Biol. Syst.* **1996**, *33*, 367−397.
(55) Anderson, M. E.; Letsinger, R. L.; Barrett, A. G. M.; Hoffman, B. M. *J. Inorg. Biochem.*, in press.